Auxin Carriers Localization Drives Auxin Accumulation in Plant Cells Infected by *Frankia* in *Casuarina glauca* Actinorhizal Nodules[1][W]

Francine Perrine-Walker[2], Patrick Doumas[2], Mikael Lucas[2], Virginie Vaissayre, Nicholas J. Beauchemin, Leah R. Band, Jérome Chopard, Amandine Crabos, Geneviève Conejero, Benjamin Péret, John R. King, Jean-Luc Verdeil, Valérie Hocher, Claudine Franche, Malcolm J. Bennett, Louis S. Tisa, and Laurent Laplaze*

UMR DIAPC, Institut de Recherche pour le Développement, 34394 Montpellier cedex 5, France (F.P.-W., P.D., V.V., A.C., B.P., V.H., C.F., L.L.); Centre for Plant Integrative Biology, University of Nottingham, Loughborough LE12 5RD, United Kingdom (M.L., L.R.B., B.P., J.R.K., M.J.B.); Department of Cellular, Molecular and Biomedical Sciences, University of New Hampshire, Durham, New Hampshire 03824–2617 (N.J.B., L.S.T.); UMR DAP, Institut National de Recherche en Informatique et Automatique, 34392 Montpellier cedex 5, France (J.C.); and Plate-forme d'Histocytologie et d'Imagerie cellulaire Végétale, Centre International de Recherche en Agronomie pour le Développement, 34392 Montpellier cedex 5, France (G.C., J.-L.V.)

Actinorhizal symbioses are mutualistic interactions between plants and the soil bacteria *Frankia* that lead to the formation of nitrogen-fixing root nodules. Little is known about the signaling mechanisms controlling the different steps of the establishment of the symbiosis. The plant hormone auxin has been suggested to play a role. Here we report that auxin accumulates within *Frankia*-infected cells in actinorhizal nodules of *Casuarina glauca*. Using a combination of computational modeling and experimental approaches, we establish that this localized auxin accumulation is driven by the cell-specific expression of auxin transporters and by *Frankia* auxin biosynthesis in planta. Our results indicate that the plant actively restricts auxin accumulation to *Frankia*-infected cells during the symbiotic interaction.

Actinorhizal symbioses are mutualistic associations between plants belonging to eight angiosperm families collectively called actinorhizal plants and the soil actinomycete *Frankia*. These interactions culminate with the formation of a new root organ, the actinorhizal nodule, where *Frankia* is hosted and fixes atmospheric nitrogen (Benson and Silvester, 1993). During intracellular infection (e.g. in *Casuarina glauca* or *Alnus glutinosa*), diffusible signals are emitted by *Frankia* at early stages of the interaction leading to root hair deformation. The chemical nature of these signals remains unknown but biochemical and genetic studies suggest that they are different from rhizobial Nod factors (Cérémonie et al., 1998; Normand et al., 2007). *Frankia* then infects some of the deformed root hairs through intracellular infection threads. A limited number of cell divisions are induced in the cortex close to the infection site leading to the formation of the prenodule. *Frankia* infects some prenodule cells and starts fixing nitrogen while new cell divisions occur in the pericycle close to a xylem pole forming a nodule primordium (Pawlowski and Bisseling, 1996). The nodule primordium subsequently grows and become infected with intracellular *Frankia* hyphae coming from the prenodule. Actinorhizal nodules have a central vasculature and the cortical symbiotic tissues containing infected and uninfected cells. Unlike legume nodules, actinorhizal nodules are structurally and developmentally related to lateral roots (Pawlowski and Bisseling, 1996).

Little is known about the signals exchanged between the two partners during the establishment of actinorhizal symbioses. The phytohormone auxin controls many developmental processes and has also been involved in plant-microbe interactions (Robert-Seilaniantz et al., 2007; Mathesius, 2008; Kazan and Manners, 2009). Recently, we studied the role of auxin influx activity during actinorhizal symbioses. Inhibition of auxin influx using the competitive inhibitor naphtoxyacetic acid perturbs actinorhizal nodule formation in *C. glauca* (Péret et al., 2007). Two genes encoding putative auxin influx carriers from *C. glauca* were cloned and characterized. One of these genes named *CgAUX1* was shown to encode a functional auxin influx carrier by complementation of the Arabidopsis (*Arabidopsis thaliana*) *aux1*

[1] This work was supported by the Institut de Recherche pour le Développement, the Agropolis Foundation (grant no. 07024), Hatch grant NH530, and the Agence Nationale de la Recherche (grant no. ANR–08–JCJC–0070–01). L.L. is supported by the Région Languedoc-Roussillon (grant "Chercheur d'Avenir").

[2] These authors contributed equally to the article.

* Corresponding author; e-mail laurent.laplaze@ird.fr.

The author responsible for distribution of materials integral to the findings presented in this article in accordance with the policy described in the Instructions for Authors (www.plantphysiol.org) is: Laurent Laplaze (laurent.laplaze@ird.fr).

[W] The online version of this article contains Web-only data.

www.plantphysiol.org/cgi/doi/10.1104/pp.110.163394

mutant. Interestingly, *CgAUX1* is expressed in *Frankia*-infected cells during actinorhizal nodule formation (Péret et al., 2007). These results together with previous data showing auxin production by *Frankia* suggest a role for auxin in infected cells during the symbiotic interaction (Mathesius, 2008; Péret et al., 2008; Grunewald et al., 2009).

The aim of this work was to further explore the involvement of auxin in the *C. glauca-Frankia* actinorhizal symbiosis. Using a combination of computational modeling and molecular and cell biology approaches, we establish that the cell-specific expression of auxin transporters leads to localized auxin accumulation in *Frankia*-infected cells in *C. glauca* nodules.

RESULTS

Auxin Accumulates in *Frankia*-Infected Cells in Actinorhizal Nodules of *C. glauca*

Previous reports suggested that the plant hormone auxin might be involved in the establishment of actinorhizal symbioses (Hammad et al., 2003; Péret et al., 2007). To study the involvement of auxin in the *C. glauca-Frankia* symbiotic interaction, we used liquid chromatography mass spectrometry (LC-MS) to quantify three major forms of auxin: indole-3-acetic acid (IAA), phenylacetic acid (PAA), and indole-3-butyric acid (IBA) in roots of plant that were not inoculated by *Frankia* (control), in root portions of inoculated plants that did not bear nodules, and in nodules 3 weeks after inoculation. In four independent experiments, the levels of all three auxins were significantly increased in roots of inoculated plants compared to control plants (Fig. 1A). Moreover, a dramatic increase in PAA content was observed in nodules compared to roots (Fig. 1A). These auxin quantification results show that IAA and PAA are the two major forms of auxins present in *C. glauca* nodules and that the symbiotic interaction with *Frankia* leads to increased PAA accumulation in plant tissues.

To localize the sites of auxin accumulation in actinorhizal nodules, we generated transgenic *C. glauca* and *Allocasuarina verticillata* plants containing the molecular markers for auxin perception Pro_{GH3}-*GUS* (Hagen et al., 1991), Pro_{DR5}-*GUS* (Ulmasov et al., 1997), or Pro_{IAA2}-*GUS* (Swarup et al., 2001). GH3 is an auxin-responsive gene from soybean (*Glycine max*) and the Pro_{GH3}-*GUS* marker has been successfully used to study changes in auxin distribution during legume nodule formation (Mathesius et al., 1998). DR5 is a synthetic auxin-responsive promoter derived from *GH3* (Ulmasov et al., 1997), and *IAA2* is an auxin-induced Arabidopsis gene. Both Pro_{DR5}-*GUS* and Pro_{IAA2}-*GUS* are commonly used as markers to analyze changes in auxin perception in Arabidopsis. In transgenic *Casuarinaceae*, those markers exhibited very weak basal levels of expression, and were not or very weakly induced by exogenous auxin (Supplemental Fig. S1). No expression was found in nodules. These results indicate that these molecular markers cannot be used in *Casuarinaceae* trees. Therefore, an immunolocalization approach was used to investigate the distribution of IAA and PAA within *C. glauca* nodules. For Arabidopsis, IAA immunolocalization was shown to reflect total auxin distribution (conjugated and free IAA), while Pro_{DR5}-*GUS* reveals sites of free auxin perception (Aloni et al., 2003; de Reuille et al., 2006). In *C. glauca* nodules, a specific monoclonal IAA antibody binds strongly to *Frankia*-infected cells (Fig. 1B). Similarly, a polyclonal PAA antibody revealed high levels of PAA accumulation in these cells (Fig. 1C). No significant hybridization was found with the IAA or PAA antibody in uninfected cells in the nodule cortex. Some binding was detected in vascular tissues with the IAA antibody. No signal was detected under the following control conditions: hybridization with only the secondary antibody (Fig. 1D), pretreatment with ethanol to remove auxin, or auxin saturation of the antibody. These results indicate that both IAA and PAA accumulate in *Frankia*-infected cells of *C. glauca* nodules. This conclusion is supported by the recent finding that *EuNOD-ARP1*, a gene from the actinorhizal plant *Eleagnus umbellata* shown to be auxin inducible in leaves, is expressed in *Frankia*-infected cells in nodules (Kim et al., 2007).

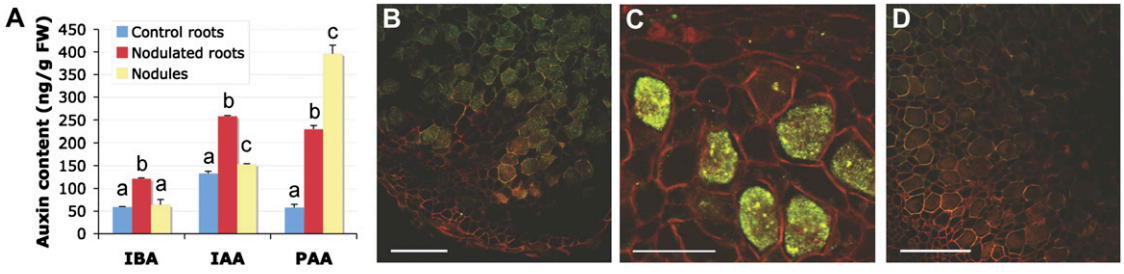

Figure 1. Auxin accumulates in *Frankia*-infected cells in *C. glauca* nodules. A, Auxin content measured by LC-MS in *C. glauca* roots of noninoculated plants (control), roots, and nodules harvested 3 weeks after inoculation by *Frankia*. Significance was tested by an ANOVA test ($P < 0.01$). FW, Fresh weight. B, Immunolocalization of IAA. The signal is found in cells infected by *Frankia*. C, Immunolocalization of PAA. A very strong signal is detected in cells infected by *Frankia*. D, Control immunolocalization. The section was hybridized only with the secondary antibody. No signal is detected in infected cells. Autofluorescence of the cell wall of infected cells can be detected. Scale bars: 100 μm (B and D), 50 μm (C).

Distribution of Auxin Carriers Predicts Auxin Accumulation in *Frankia*-Infected Cells of *C. glauca* Nodules

We previously found that the *CgAUX1* gene that encodes an auxin influx carrier functionally equivalent to Arabidopsis AtAUX1 is expressed in the vascular tissues and in *Frankia*-infected cells in *C. glauca* nodules (Péret et al., 2007). To test whether this *CgAUX1* expression might be sufficient to explain the pattern of auxin accumulation, we used a computational modeling approach similar to the ones that have been applied successfully to study developmental processes such as phyllotaxis (de Reuille et al., 2006; Chickarmane et al., 2010). Auxin fluxes and accumulation patterns in a tissue can be inferred from the cellular localization of transporters.

We generated cellular models for auxin transport occurring in *C. glauca* nodule symbiotic tissues. First, the cortical tissue of *C. glauca* nodules was observed to have a very specific geometry and topology (Supplemental Fig. S2). For instance, infected cells (easily detected using *Frankia* autofluorescence or 4′,6-diaminophenylindole staining) were bigger (5–10 times) and more connected, i.e. were in contact with more cells, than noninfected cells (mean connectivity, i.e. number of contact with other cells, was 6.99 and 4.99, respectively). Because of the infection mechanism, infected cells tend to be organized in files. Thus, confocal images of *C. glauca* nodules were digitized and used to generate our virtual tissues to keep the specific geometry and topology since fluxes are known to be dependent on those properties. Three in silico models of cortical tissues were generated from confocal images of three different nodules (Fig. 2A; Supplemental Fig. S2). Two different cell types corresponding to infected and uninfected cells were defined in the virtual tissues.

After the addition of AUX1-like auxin influx carrier activity to the infected cells in the in silico model, the dynamic of auxin distribution was tested in the three virtual tissues. Simulations were conducted with either auxin initially homogeneously distributed in the tissue or with auxin coming from the outside of the tissue (as would be the case if auxin was provided by the vascular stream). In all our simulations, the addition of AUX1 activity in infected cells was not sufficient to generate a significant auxin accumulation in infected cells (Fig. 2B; Supplemental Fig. S3). This result suggests that other components are needed to generate a specific auxin accumulation in *Frankia*-infected cells.

A search of a *C. glauca* EST database (Hocher et al., 2006), currently containing around 35,000 ESTs, for other auxin transport proteins that might be active in nodules identified one EST corresponding to an auxin efflux carrier of the PIN family (EST CG-R02f_005_F13 homologous to PIN1 and named *CgPIN1* thereafter) and 20 ESTs corresponding to the previously described putative auxin influx carriers CgAUX1 and CgLAX3 (Péret et al., 2007). Expression analyses showed that *CgPIN1* and *CgLAX3* were down-regulated 2.5 and more than 16 times, respectively, in nodules compared to uninfected roots (Fig. 2C). *CgAUX1* expression was not significantly different in nodules compared to uninfected roots (Fig. 2C). In conclusion, we identified genes encoding an auxin influx carrier (*CgAUX1*) and a putative auxin efflux carrier (*CgPIN1*) expressed in *C. glauca* nodules.

To determine the localization of PIN1-like proteins in *C. glauca* nodules, we performed immunolocalization experiments using polyclonal anti-AtPIN1 antibodies that have been previously shown to detect PIN1-like proteins in Arabidopsis and maize (*Zea mays*; Carraro et al., 2006). We found a strong signal occurring in the membrane of uninfected cortical cells surrounding *Frankia*-infected cells in *C. glauca* nodules (Fig. 2, D–G). This signal was strongest in the apical region of the nodule close to the nodule meristem (Fig. 2D) and appeared all around the periphery of cells, suggesting that auxin transport was not polarized (Fig. 2, F and H). Some signal was also found in the vasculature close to the meristem. Thus in *C. glauca* nodules, noninfected cortical cells expressed a gene encoding a PIN1-like auxin efflux carrier, while infected cells expressed a gene encoding an auxin influx carrier (*CgAUX1*). While we cannot rule out that other transporters might be involved in auxin transport in the cortical tissue, no other EST corresponding to an auxin carrier was found in our database that contains 35,000 *C. glauca* ESTs (including 15,000 ESTs from nodule).

The effects of these auxin influx and efflux carrier activities in infected and uninfected cells, respectively, were tested in our virtual symbiotic tissues model system. We found in our three in silico models that this cell-specific localization of auxin transporters was sufficient to cause a rapid auxin accumulation specifically in *Frankia*-infected cells (Fig. 2I; Supplemental Fig. S4) as was observed in our auxin immunolocalization experiments. This prediction was very robust and held for a wide range of parameter values (Supplemental Fig. S5).

Frankia Is a Potential Source of Auxin Production during the Symbiotic Association

In our models, if auxin was supplied from outside the tissue it accumulated in those infected cells that were close to the auxin source (Supplemental Fig. S4). This prediction is in disagreement with our immunolocalization results that showed strong signal in all of the infected cells irrespective of their position in the symbiotic tissues. This inconsistency suggests that auxin comes from within symbiotic tissues rather than from an external source.

Auxin production has been demonstrated for several different *Frankia* strains, but not strain CcI3 (Wheeler et al., 1984; Berry et al., 1989; Hammad et al., 2003). IAA, IBA, and PAA production by the *C. glauca*-infective *Frankia* strain CcI3 was quantified by LC-MS analysis of the supernatant from in vitro cultures. Although *Frankia* CcI3 cultivated in BAP

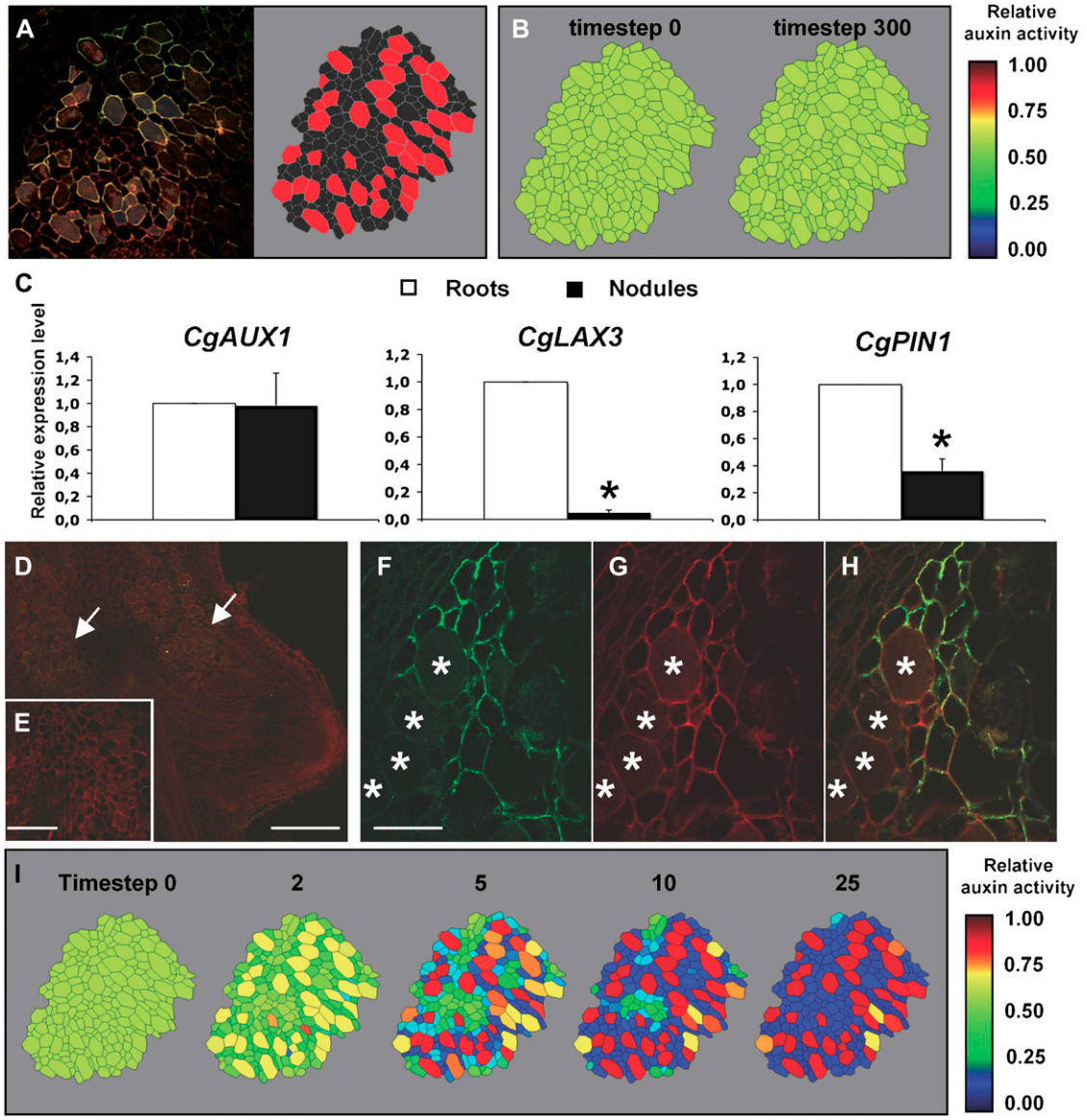

Figure 2. Expression of auxin transporters in *C. glauca* nodules is sufficient to predict an auxin accumulation in *Frankia*-infected cells. A, Example of digitization of nodule tissue. Confocal microscopy images of nodule tissue autofluorescence (left section) were used as a base for manual digitization of the geometry in a virtual representation of the nodule (right section, see also Supplemental Fig. S1). Information regarding the infection of the cells was added in the virtual tissue (infected cells here denoted in red). B, Distribution of auxin in a virtual nodule with infected cells expressing *CgAUX1*, starting from a uniform auxin level. Infected cells accumulate auxin very slowly in this condition (see Supplemental Fig. S2 for other virtual nodules and starting auxin distribution). Auxin activity is the relative auxin concentration within the cells and its representation is capped at value 1. C, Expression of *CgAUX1*, *CgLAX3*, and *CgPIN1* in *C. glauca* uninfected roots and nodules harvested 3 weeks after inoculation. RNA abundance was determined by qRT-PCR and presented are means ± SD of three independent experiments. $*P < 0.05$, Statistical randomization test (Rest 2009 software; Qiagen). D to H, Immunolocalization of PIN1-like proteins in *C. glauca* nodules. D, PIN1-like proteins are detected (arrows) close to the nodule apex, i.e. in the region close to the meristem. E, No signal was detected in control immunolocalization experiments without the PIN1. F to H, Close-up in the apex of a *C. glauca* nodule showing the signal corresponding to the PIN1 antibody (F), autofluorescence (G), and the merged image (H). Infected cells are marked with asterisks. I, Evolution of the distribution of auxin in a virtual nodule with infected cells expressing *CgAUX1* and noninfected cells expressing *CgPIN1*, starting from a uniform auxin level. Auxin activity is the relative auxin concentration within the cells and its representation is capped at value 1. The generated auxin distribution was shown to be robust to CgPIN1 perturbation (see Supplemental Fig. S4). Scale bars: 250 μm (D), 100 μm (E), and 50 μm (F–H).

medium produced all three auxin types, IAA and PAA were the dominant forms of auxin and IBA was minor form (<2% of the pool; Fig. 3A). *Frankia* CcI3 growth in BAP medium without nitrogen source caused a significant increase in IAA and PAA production (Fig. 3A). A >3-fold increase in PAA production was detected under these conditions. These results indicate that auxin production by *Frankia* CcI3 in vitro is dependent on the nitrogen status and that PAA may be the major form biosynthesized.

The availability of several *Frankia* genome databases including *Frankia* CcI3 (Normand et al., 2007) allowed a genome-mining approach to identify genes potentially involved in auxin biosynthesis and transport. All of the *Frankia* genomes contained predicted genes for complete indole-3-pyruvate and phenyl pyruvate pathways for IAA and PAA biosynthesis, respectively (Fig. 3B). Since many beneficial plant-associated bacteria preferentially use the indole-3-pyruvate pathway for IAA biosynthesis (Spaepen et al., 2007), this result is not surprising. *Frankia* CcI3 orthologs were identified for the three key enzymes in the indole-3-pyruvate and the phenyl pyruvate pathways. Interestingly, most of these genes were found by quantitative reverse transcription (qRT)-PCR to be overexpressed when bacteria were grown in BAP medium without nitrogen source (Fig. 3, B and C), i.e. under conditions that caused a significant increase in IAA and PAA production. A gene encoding a putative microbial auxin efflux carrier (Francci3_1249) was also identified from the automatic annotation of *Frankia* CcI3 and orthologs were found in all *Frankia* genomes. RT-PCR experiments showed that these genes were expressed in *Frankia* grown in vitro and in *C. glauca* nodules (Fig. 4), suggesting that *Frankia* IAA and PAA biosynthetic pathways are active in planta.

Auxin biosynthesis by *Frankia* was included in our in silico model as a source of auxin. This modification led to a rapid accumulation of auxin in all infected plant cells (Fig. 5). If CgPIN1 activity is removed in this new model, auxin accumulation occurs both in infected cells and in neighboring uninfected cells (Fig. 5). On the other hand, we did not observe any effect after removing CgAUX1 activity in the model. This result suggests that *CgPIN1* is necessary to restrict auxin accumulation to plant cells infected by *Frankia*.

DISCUSSION

Two nitrogen-fixing root nodule symbioses between plants and bacteria have been described, actinorhizal symbioses, formed by members of the Fagales, Rosales, and Cucurbitales with *Frankia* bacteria, and the interaction of legumes with rhizobia. Both symbioses involve intracellular accommodation of bacteria within host cells. While symbiotic signaling mechanisms have been widely studied in the legume-rhizobia symbiosis (Oldroyd et al., 2009) very little is known about signaling mechanisms involved in plant-bacteria recognition in actinorhizal symbioses. Previous studies have suggested a role for auxin in the

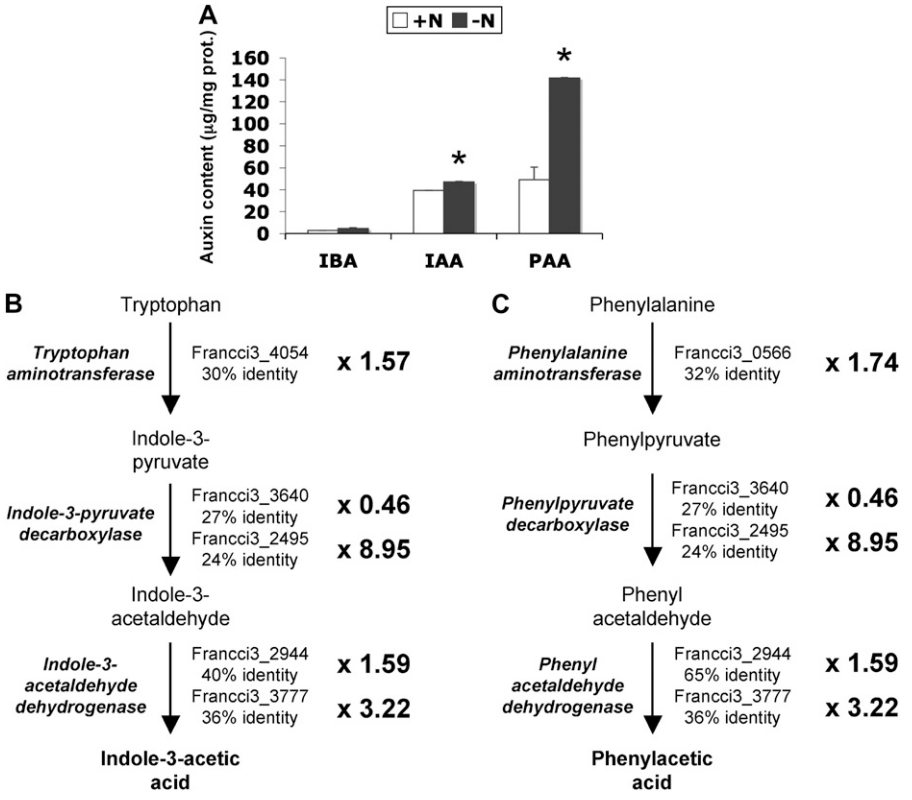

Figure 3. Auxin production by *Frankia*. A, Auxin content measured by LC-MS in the supernatant of in vitro *Frankia* CcI3 cultures. Bacteria were grown in BAP medium with (+N) or without (−N) nitrogen sources. Data are means ± SD. Significance was tested by an ANOVA test. * $P < 0.01$ compared with noninoculated. B to C, Putative IAA (B) and PAA (C) biosynthetic pathways identified in *Frankia* CcI3 using genome data mining. *Frankia* CcI3 orthologs were identified for the three key enzymes in the indole-3-pyruvate and the phenyl pyruvate pathways (see Supplemental Table S1). Expression of the corresponding genes in *Frankia* CcI3 bacteria grown in BAP medium with or without a nitrogen source was analyzed by qRT-PCR. Fold changes values represent the mean ratios of expression changes in BAP−N relative to BAP+N medium in two independent biological replicates.

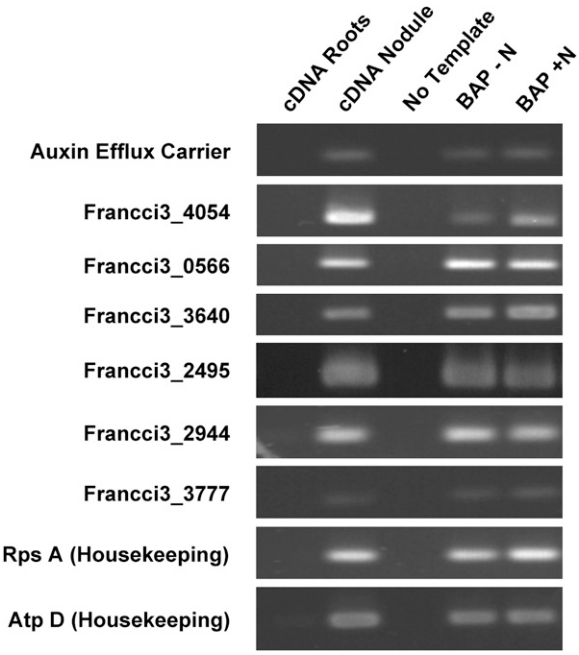

Figure 4. Expression of *Frankia* genes in the putative IAA and PAA pathways. Expression of the corresponding genes was tested in culture and in plant tissues using RT-PCR. All of the *Frankia* CcI3 putative IAA and PAA biosynthetic genes were expressed in culture and in planta, but were not expressed in plant root tissues. Furthermore, the two housekeeping genes and the auxin efflux carrier were expressed under these conditions.

establishment of actinorhizal symbioses (Hammad et al., 2003; Péret et al., 2007, 2008). Here, we report that auxin accumulates in cortical cells infected by *Frankia* in *C. glauca* nodules. This result is in agreement with the expression of the auxin-responsive *EuNOD-ARP1* gene in *Frankia*-infected cells in *E. umbellata* actinorhizal nodules (Kim et al., 2007) and with the expression of an auxin-responsive AUX/IAA gene in *Frankia*-infected cells in *C. glauca* nodules (V. Vaissayre, A. Crabos, V. Hocher, A. Champion, and L. Laplaze, unpublished data). These results together further indicate that auxin-responsive genes are activated in infected cells and therefore that at least part of the auxin we detected using immunolocalization is active.

Results from a combination of experimental biology and computational modeling approaches indicate that this specific accumulation of auxin in *Frankia*-infected cell is driven by auxin import into infected cells by expression of *AUX1* in these cells, and auxin export from uninfected cells by expression of a PIN1-like gene in those cells. Our data also suggest that *Frankia* produces auxins (both IAA and PAA) in planta, but our data do not allow us to conclude that *Frankia* is the only source of auxin in nodules. Although *Frankia* mutant strains defective in auxin biosynthesis would be very helpful to clarify this point, techniques to generate stable transgenic or mutant *Frankia* strains have not yet been established (Lavire and Cournoyer, 2003).

However, it is clear that the arrangement of auxin transporters limits the auxin response to those cells that are infected by *Frankia* and prevents the diffusion of this very active biomolecule to other nodule tissues or parts of the plant. This localization raises the question of the role of auxin in infected cells and we propose three potential functions. First, auxin accumulation in infected cells could drive cell growth and help explain why infected cells are hypertrophied. Another potential role for auxin is cell wall remodeling processes that occur during infection. The infection threads are surrounded by the plant cell membrane and a new cell wall-like structure composed mainly of pectin derivatives (Lalonde and Knowles, 1975). Auxin is known to regulate genes involved in cell wall remodeling, pectin biosynthesis, and methylation (Lerouxel et al., 2006; Swarup et al., 2008). Thus, auxin perception in infected plant cells might be necessary for the growth of the infection threads. Finally, auxin could be involved in preventing, controlling, or limiting the plant defense mechanisms. Some bacterial pathogens such as *Pseudomonas syringae* modulate auxin responses and/or production to colonize their host (Chen et al., 2007; Robert-Seilaniantz et al., 2007; Kazan and Manners, 2009). A similar process might occur in *C. glauca* cells infected by *Frankia*.

A role for auxin in infected cells might not be a general feature of nitrogen-fixation endosymbioses. While the role of auxin in legume nodule development is now well documented (Mathesius, 2008), little is known about its role in the infection process. Although legume infection by rhizobia strain deficient in IAA production or overproducing auxin causes changes in nodule development and nitrogen fixation (Pii et al., 2007; Camerini et al.,

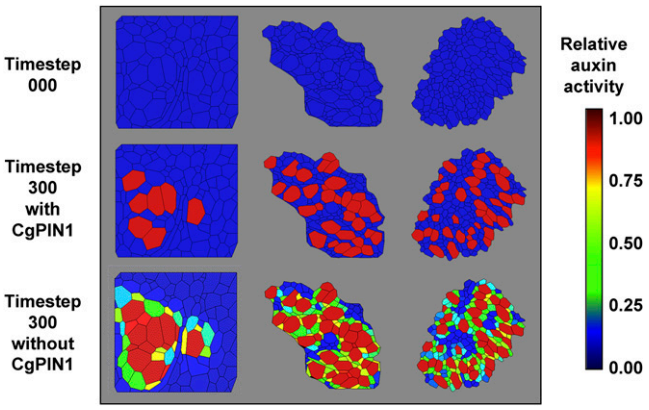

Figure 5. Simulation of auxin distribution in virtual tissues with auxin synthesis by *Frankia*. We considered an additional intracellular compartment in infected cell in which *Frankia* would release auxin. Simulation showed that it would lead to auxin accumulation specifically in infected cells provided that CgPIN1 was expressed in the noninfected cell. Auxin activity is the relative auxin concentration within the cells and its representation is capped at value 1. The equations that govern diffusive and active transport are discussed in detail in Supplemental Text S1 (model notes).

2008), the molecular markers of auxin perception Pro_{DR5}-*GUS* and Pro_{GH3}-*GUS* are not expressed in infected cells of legume nodules (Mathesius et al., 1998; Pacios-Bras et al., 2003) and no data on auxin immunolocalization are available. It thus remains to be shown whether auxin accumulation is a common feature of endosymbiotic infection of plant cells by nitrogen-fixing bacteria.

MATERIALS AND METHODS

Plant and Bacterial Material

Casuarina glauca seeds were provided by Carter Seeds and grown as described in Péret et al. (2007). Transgenic *C. glauca* and *Allocasuarina glauca* plants were produced and analyzed as described (Péret et al., 2007). *Frankia* strain CcI3 was grown and used to inoculate *C. glauca*, as described (Péret et al., 2007).

Auxin Quantification

Frozen samples were ground in liquid nitrogen and auxins were extracted twice for 2 h at 4°C in the dark in 80% (v/v) methanol added with 1% butylated hydroxytoluene. For auxin quantification, 100 pmol of [$^2H_6$]IAA and 100 pmol of [^{13}C]PAA (Euriso-Top) were added to the samples. After centrifugation (13,000*g*, 20 min, 4°C), the supernatants were collected and passed through a C18 cartridge (Waters). Afterward, auxins were purified using a DEAE-Sephadex A25 cartridge (formic acid conditions; Amersham Pharmacia) coupled to C18 cartridge as described in Prinsen et al. (2000). Auxins were directly eluted from the C18 column with ethyl ether. Mass analysis was conducted using a Quattro LC with an ESI Z-spray interface (MicroMass), MassLynx software, an Alliance 2695 RP-HPLC system (Waters), and a Waters 2487 UV detector set at 280 nm. An Xterra C18 column (100 × 2 mm, 5 μm, Waters) was used with a mix comprising solvent A water with 15 mM formic acid and solvent B methanol with a gradient profile (starting with 60:40, A/B, v/v, for 2 min; linear gradient up to 0:100, A/B over 15 min; a washing step 0:100, A/B for 5 min, and final equilibration at 60:40, A/B for 5 min) at a 0.3 mL/min flow rate. Chromatograms were analyzed using the Masslynx software (Waters), and the IAA, PAA, and IBA concentrations were calculated according to the principle of isotope dilution (Prinsen et al., 1998). Samples were quantified in single reaction monitoring mode based on the area of major MS signals ([M-H$^+$]).

Auxin Immunolocalization

For IAA and PAA immunolocalization, fresh nodules sections of 50 to 60 μM were obtained with a vibratome (MicroM HM650V) and were fixed overnight, in fixative solution (4% w/v 1-ethyl-3-[3-dimethylaminopropyl]-carbodiimide hydrochloride [EDAC, Sigma], 4% w/v paraformaldehyde [Fluka] in phosphate-buffered saline [10 mM pH 7.4]) at 4°C. Sections were incubated overnight in 2% blocking buffer solution (Roche) at 4°C followed by overnight incubation with primary antibody, anti-IAA mouse monoclonal hybridoma antibody (Agdia) at a concentration of 0.05 mg/mL, or anti-PAA rabbit polyclonal antibody (Abcam) at 1:200 dilution. Sections were then rinsed (three times 15 min) in phosphate-buffered saline (10 mM pH 7.4). Alexa Fluor 488 goat anti-mouse IgG_1 (γ^1) antibody (2 mg/mL; Invitrogen) for IAA or Alexa Fluor 488 goat anti-rabbit IgG antibody (2 mg/mL; Invitrogen) for PAA was used as a secondary antibody at 1:250 dilution at room temperature during 1 h in the dark. After rinsing (five times for 10 min each), sections were mounted in Mowiol (Calbiochem) and examined using a confocal microscope 510 META Zeiss (Laser Argon 488, BP 505–530 and LP 560 nm) with LCI Neo-Neofluar 25×/0.8 1 mm Korr DIC27 and EC Plan-Neofluar 10×/0.3 objectives. For the ethanol controls, sections were pretreated with ethanol for 1 h at each concentration (70% v/v and 80% v/v in phosphate-buffered saline 10 mM pH 7.4) prior to fixation to extract IAA or PAA from the nodule sections. To verify the binding specificity of the primary anti-IAA mouse monoclonal antibody was mixed with 10 times its concentration of IAA overnight. This was to allow the binding of the free IAA to the primary antibody. The solution was applied to the fixed sections, i.e. the bound primary antibody would not be able to bind to the antigen on the sections. The same was done to test the primary anti-PAA rabbit polyclonal antibody against PAA. Another control treatment was also done whereby the secondary antibody was used alone. Nodules from 24 and 16 plants from four independent inoculation experiments were used for IAA and PAA immunolocalization, respectively.

PIN1 Immunolocalization

Fresh nodules sections of 50 to 60 μm were obtained with a vibratome (MicroM HM650V) and were fixed for 1 h in fixative solution (4% w/v paraformaldehyde [Fluka] in phosphate-buffered saline 10 mM pH 7.4) under vacuum at room temperature. Sections were incubated overnight in 2% blocking buffer solution (Roche) at 4°C followed by overnight incubation with primary antibody, anti-PIN1 goat polyclonal antibody (200 μg/mL; Santa Cruz Biotechnology) at 1:200 dilution. Sections were rinsed three times (15 min) in phosphate-buffered saline 10 mM pH 7.4. Alexa Fluor 488 F(ab')2 fragment of rabbit anti-goat IgG (H + L) antibody (2 mg/mL; Invitrogen) was used as a secondary antibody at 1:250 dilution at room temperature during 1 h in the dark. After rinsing, sections were mounted in Mowiol (Calbiochem) and examined using a Zeiss confocal microscope 510 META (Laser Argon 488, BP 505–530 and LP 560 nm) with LCI Neo-Neofluar 25×/0.8 1 mm Korr DIC27 and EC Plan-Neofluar 10×/0.3 objectives. For the control treatment, the primary antibody was not used at all.

Gene Expression Analyses

C. glauca gene expression analyses were performed by qRT-PCR using specific primers (Supplemental Table S2) as described (Gherbi et al., 2008). Reactions were preformed in triplicates and the comparative threshold-cycle method was used to quantify gene expression. The results were standardized with *CgUBI* expression levels (Gherbi et al., 2008).

Total RNA was extracted from *Frankia* as described previously (Niemann and Tisa, 2008). To study *Frankia* gene expression in planta, total RNA was extracted using the RNeasy plant mini kit (Qiagen GmbH). RNA was quantified with a NanoDrop (ThermoFisher). Four-hundred nanograms of total RNA were reverse transcribed using SuperScript III reverse transcriptase (Invitrogen) and random hexamers primers. The RT-PCR was preformed using AmpliTaq Gold 360 master mix (Applied Biosystems) and 100 ng of cDNA as a template. qPCR was performed using SYBR Green PCR master mix (Applied Biosystems) and specific primer sets (Supplemental Table S2). Parameters for the Applied Biosystems 7300 were as follows: (1) one cycle 95°C 10 min, (2) 40 cycles 95°C for 15 s and 60°C for 30 s, ended by one cycle at 95°C for 15 s, 60°C for 30 s, and 95°C for 15 s run. Reactions were preformed in triplicates and the comparative threshold-cycle method was used to quantify gene expression. The results were standardized with *rpsA* expression levels. For RT-PCR, the thermocycler parameters were as follows: (1) initial denaturation at 95°C 5 min, (2) 35 cycles of denaturation at 95°C for 30 s, primer annealing at 55°C for 30 s, and primer extension at 72°C for 30 s, and (3) a final extension step at 72°C 10 min. Amplicons were resolved by gel electrophoresis.

Modeling

Tissues were manually digitized from confocal images to standard vector graphic files (SVG) and automatically converted for use in the OpenAlea modeling software platform (Pradal et al., 2008). The models take into account cells and apoplastic compartments for computing the auxin transport (see Supplemental Text S1 for additional details). The model parameters (membrane permeability and active transports, auxin dissociation constant, cell and apoplastic pH, cell membrane potential) were defined in accordance with values from previously published studies (see Supplemental Text S1). Computational modeling was based on IAA transport parameters as they were the only auxin transport parameters that are well documented. However, our model is an abstraction of the physiology of the nodule, and as such is not tied to an auxin in particular. Similar results would be obtained for PAA assuming that IAA and PAA transport physiology are similar.

Bioinformatics Studies

The FASTA amino acid sequences of the three *Frankia* genomes (CcI3, National Center for Biotechnology Information [NCBI] RefSeq: NC_007777; ACN14a, NCBI RefSeq: NC_00827; EAN1pec, NCBI RefSeq: NC_009921 and from the three *Frankia* draft genomes [EuI1c, http://genome.ornl.gov/microbial/fran_eui1c/; EUN1f, http://genome.ornl.gov/microbial/fran_eun1f/;

the uncultured *Frankia* symbiont of *Datisca glomerata* http://genome.ornl.gov/microbial/fran_sym/]) were obtained from GenBank or the Department of Energy Joint Genome Institute Genome Portal site (http://genome.jgi-psf.org/). Functionally analyzed genes for indole acetic acid and phenyl acetic acid biosynthesis pathways were identified by the use of Kyoto Encyclopedia of Genes and Genomes (Kanehisa and Goto, 2000) and published literature (Patten and Glick, 1996; Spaepen et al., 2007). Proteins representing different biosynthesis pathways were used (Supplemental Table S1). BLASTP analyses were performed against each *Frankia* genome database using each of the above protein sequences as a query sequence for the representative IAA and PAA biosynthesis pathways.

Sequence data from this article can be found in the GenBank/EMBL data libraries under accession numbers FQ375841 (*CgPIN1*) and NC_007777.1 (*Frankia* sp. CcI3 genome).

Supplemental Data

The following materials are available in the online version of this article.

Supplemental Figure S1. Expression pattern of the Pro_{IAA2}-*GUS* molecular markers for auxin perception in *C. glauca*.

Supplemental Figure S2. Topology and digitization of symbiotic tissues.

Supplemental Figure S3. Simulation of auxin distribution in virtual tissues with infected cells expressing *CgAUX1*.

Supplemental Figure S4. Simulation of auxin distribution in virtual tissues with infected cells expressing *CgAUX1* and noninfected cells expressing *CgPIN1*.

Supplemental Figure S5. Robustness of auxin distribution against CgPIN1 perturbation.

Supplemental Table S1. Genome data mining results.

Supplemental Table S2. Primers used for gene expression analyses.

Supplemental Text S1. Model description.

ACKNOWLEDGMENTS

We thank Pr. K. Ljung (Swedish University of Agricultural Sciences, Umea, Sweden) for providing us with [$^2H_6$]IAA, Pr. T. Guilfoyle (University of Missouri) for the Pro_{DR5}-*GUS* and Pro_{GH3}-*GUS* constructs, and Dr. R. Swarup (University of Nottingham, UK) for the Pro_{IAA2}-*GUS* construct. We are grateful to Dr. D. Bogusz (Institut de Recherche pour le Développement, France), Dr. A. Champion (Institut de Recherche pour le Développement, France), Dr. S. Guyomarc'h (Université Montpellier 2, France), and Dr. C. Godin (Institut National de Recherche en Informatique et Automatique, France) for helpful discussions and critical reading of this manuscript.

Received July 26, 2010; accepted September 4, 2010; published September 8, 2010.

LITERATURE CITED

Aloni R, Schwalm K, Langhans M, Ullrich CI (2003) Gradual shifts in sites of free-auxin production during leaf-primordium development and their role in vascular differentiation and leaf morphogenesis in Arabidopsis. Planta **216:** 841–853

Benson DR, Silvester WB (1993) Biology of *Frankia* strains, actinomycete symbionts of actinorhizal plants. Microbiol Rev **57:** 293–319

Berry AM, Kahn RKS, Booth MC (1989) Identification of indole compounds secreted by *Frankia* HFPAri3 in defined culture-medium. Plant Soil **118:** 205–209

Camerini S, Senatore B, Lonardo E, Imperlini E, Bianco C, Moschetti G, Rotino GL, Campion B, Defez R (2008) Introduction of a novel pathway for IAA biosynthesis to rhizobia alters vetch root nodule development. Arch Microbiol **190:** 67–77

Carraro N, Forestan C, Canova S, Traas J, Varotto S (2006) *ZmPIN1a* and *ZmPIN1b* encode two novel putative candidates for polar auxin transport and plant architecture determination of maize. Plant Physiol **142:** 254–264

Cérémonie H, Cournoyer B, Maillet F, Normand P, Fernandez MP (1998) Genetic complementation of rhizobial *nod* mutants with *Frankia* DNA: artifact or reality? Mol Gen Genet **260:** 115–119

Chen Z, Agnew JL, Cohen JD, He P, Shan L, Sheen J, Kunkel BN (2007) *Pseudomonas syringae* type III effector AvrRpt2 alters *Arabidopsis thaliana* auxin physiology. Proc Natl Acad Sci USA **104:** 20131–20136

Chickarmane V, Roeder AH, Tarr PT, Cunha A, Tobin C, Meyerowitz EM (2010) Computational morphodynamics: a modeling framework to understand plant growth. Annu Rev Plant Biol **61:** 65–87

de Reuille PB, Bohn-Courseau I, Ljung K, Morin H, Carraro N, Godin C, Traas J (2006) Computer simulations reveal properties of the cell-cell signaling network at the shoot apex in Arabidopsis. Proc Natl Acad Sci USA **103:** 1627–1632

Gherbi H, Markmann K, Svistoonoff S, Estevan J, Autran D, Giczey G, Auguy F, Péret B, Laplaze L, Franche C, et al (2008) SymRK defines a common genetic basis for plant root endosymbioses with arbuscular mycorrhiza fungi, rhizobia, and *Frankia* bacteria. Proc Natl Acad Sci USA **105:** 4928–4932

Grunewald W, van Noorden G, Van Isterdael G, Beeckman T, Gheysen G, Mathesius U (2009) Manipulation of auxin transport in plant roots during *Rhizobium* symbiosis and nematode parasitism. Plant Cell **21:** 2553–2562

Hagen G, Martin G, Li Y, Guilfoyle TJ (1991) Auxin-induced expression of the soybean *GH3* promoter in transgenic tobacco plants. Plant Mol Biol **17:** 567–579

Hammad Y, Nalin R, Marechal J, Fiasson K, Pepin R, Berry AM, Normand P, Domenach A-M (2003) A possible role for phenyl acetic acid (PAA) on *Alnus glutinosa* nodulation by *Frankia*. Plant Soil **254:** 193–205

Hocher V, Auguy F, Argout X, Laplaze L, Franche C, Bogusz D (2006) Expressed sequence-tag analysis in *Casuarina glauca* actinorhizal nodule and root. New Phytol **169:** 681–688

Kanehisa M, Goto S (2000) KEGG: kyoto encyclopedia of genes and genomes. Nucleic Acids Res **28:** 27–30

Kazan K, Manners JM (2009) Linking development to defense: auxin in plant-pathogen interactions. Trends Plant Sci **14:** 373–382

Kim HB, Lee H, Oh CJ, Lee NH, An CS (2007) Expression of *EuNOD-ARP1* encoding auxin-repressed protein homolog is upregulated by auxin and localized to the fixation zone in root nodules of *Elaeagnus umbellata*. Mol Cells **23:** 115–121

Lalonde M, Knowles R (1975) Ultrastructure, composition, and biogenesis of encapsulation material surrounding endophyte in *Alnus crispa* var Mollis root nodules. Can J Bot **53:** 1951–1971

Lavire C, Cournoyer B (2003) Progress on the genetics of the N-2-fixing actinorhizal symbiont Frankia. Plant Soil **254:** 125–137

Lerouxel O, Cavalier DM, Liepman AH, Keegstra K (2006) Biosynthesis of plant cell wall polysaccharides—a complex process. Curr Opin Plant Biol **9:** 621–630

Mathesius U (2008) Auxin: at the root of nodule development? Funct Plant Biol **35:** 651–668

Mathesius U, Schlaman HRM, Spaink HP, Of Sautter C, Rolfe BG, Djordjevic MA (1998) Auxin transport inhibition precedes root nodule formation in white clover roots and is regulated by flavonoids and derivatives of chitin oligosaccharides. Plant J **14:** 23–34

Niemann J, Tisa LS (2008) Nitric oxide and oxygen regulate truncated hemoglobin gene expression in *Frankia* strain CcI3. J Bacteriol **190:** 7864–7867

Normand P, Lapierre P, Tisa LS, Gogarten JP, Alloisio N, Bagnarol E, Bassi CA, Berry AM, Bickhart DM, Choisne N, et al (2007) Genome characteristics of facultatively symbiotic *Frankia* sp. strains reflect host range and host plant biogeography. Genome Res **17:** 7–15

Oldroyd GE, Harrison MJ, Paszkowski U (2009) Reprogramming plant cells for endosymbiosis. Science **324:** 753–754

Pacios-Bras C, Schlaman HR, Boot K, Admiraal P, Langerak JM, Stougaard J, Spaink HP (2003) Auxin distribution in *Lotus japonicus* during root nodule development. Plant Mol Biol **52:** 1169–1180

Patten CL, Glick BR (1996) Bacterial biosynthesis of indole-3-acetic acid. Can J Microbiol **42:** 207–220

Pawlowski K, Bisseling T (1996) Rhizobial and actinorhizal symbioses: what are the shared features? Plant Cell **8:** 1899–1913

Péret B, Svistoonoff S, Lahouze B, Auguy F, Santi C, Doumas P, Laplaze L (2008) A role for auxin during actinorhizal symbioses formation? Plant Signal Behav **3:** 34–35

Péret B, Swarup R, Jansen L, Devos G, Auguy F, Collin M, Santi C, Hocher V, Franche C, Bogusz D, et al (2007) Auxin influx activity is associated with *Frankia* infection during actinorhizal nodule formation in *Casuarina glauca*. Plant Physiol **144:** 1852–1862

Pii Y, Crimi M, Cremonese G, Spena A, Pandolfini T (2007) Auxin and nitric oxide control indeterminate nodule formation. BMC Plant Biol **7:** 21

Pradal C, Dufour-Kowalski S, Boudon F, Fournier C, Godin C (2008) OpenAlea: a visual programming and component-based software platform for plant modelling. Funct Plant Biol **35:** 751–760

Prinsen E, Van Dongen W, Esmans EL, Van Onckelen HA (1998) Micro and capillary liquid chromatography tandem mass spectrometry: a new dimension in phytohormone research. J Chromatogr A **826:** 25–37

Prinsen E, Van Laer S, Oden S, Van Onckelen H (2000) Auxin analysis. Methods Mol Biol **141:** 49–65

Robert-Seilaniantz A, Navarro L, Bari R, Jones JD (2007) Pathological hormone imbalances. Curr Opin Plant Biol **10:** 372–379

Spaepen S, Vanderleyden J, Remans R (2007) Indole-3-acetic acid in microbial and microorganism-plant signaling. FEMS Microbiol Rev **31:** 425–448

Swarup K, Benková E, Swarup R, Casimiro I, Péret B, Yang Y, Parry G, Nielsen E, De Smet I, Vanneste S, et al (2008) The auxin influx carrier LAX3 promotes lateral root emergence. Nat Cell Biol **10:** 946–954

Swarup R, Friml J, Marchant A, Ljung K, Sandberg G, Palme K, Bennett M (2001) Localization of the auxin permease AUX1 suggests two functionally distinct hormone transport pathways operate in the Arabidopsis root apex. Genes Dev **15:** 2648–2653

Ulmasov T, Murfett J, Hagen G, Guilfoyle TJ (1997) Aux/IAA proteins repress expression of reporter genes containing natural and highly active synthetic auxin response elements. Plant Cell **9:** 1963–1971

Wheeler CT, Crozier A, Sandberg G (1984) The biosynthesis of indole-3-acetic-acid by *Frankia*. Plant Soil **78:** 99–104